Available online at www.sciencedirect.com
ScienceDirect
Chemosphere 69 (2007) 262–270
CHEMOSPHERE
www.elsevier.com/locate/chemosphere

Immobilization of polyphenol oxidase onto mesoporous activated carbons – isotherm and kinetic studies

L. John Kennedy, P.K. Selvi, Aruna Padmanabhan, K.N. Hema, G. Sekaran *

Department of Environmental Technology, Central Leather Research Institute, Adyar, Chennai 600 020, India

Received 13 September 2005; received in revised form 27 March 2007; accepted 2 April 2007
Available online 1 June 2007

Abstract

Investigations were carried out in batch modes for studying the immobilization behavior of polyphenol oxidase (PPO) on two different mesoporous activated carbon matrices, MAC400 and MAC200. The PPO was immobilized onto MAC400 and MAC200 at various enzyme activities 5×10^4, 10×10^4, 20×10^4, 30×10^4 U l^{-1}, at pH 5–8, and at temperature ranging from 10 to 40 °C. The intensity of immobilization of PPO increased with increase in temperature and initial activities, while it decreased with increase in pH. Immobilization onto MAC400 followed the Langmuir model while Langmuir and Freundlich models could fit MAC200 data. Non-linear pseudo first order, pseudo second order and intraparticle diffusion models were evaluated to understand the mechanism of immobilization. The free and immobilized enzyme kinetic parameters (K_m and V_{max}) were determined by Michaelis–Menten enzyme kinetics. The K_m values for free enzyme, PPO immobilized in MAC400 and in MAC200 were 0.49, 0.41 and 0.65 mM, respectively. The immobilization of PPO in carbon matrices was confirmed using FT-IR spectroscopy and scanning electron microscopy.

Keywords: Immobilization; Polyphenol oxidase; Mesoporous activated carbon; Adsorption isotherms; Kinetic models

1. Introduction

Enzymes are biocatalysts with high specificity, high catalytic efficiency and bio-degradability and hence find major application in industrial sectors and in medical sciences as they increase the rate of chemical reaction by lowering the activation energy (Palmer, 1991). However, their effective use is restricted because of certain properties like non-reusability, instability, high cost and sensitivity to denaturation. These restrictions, which remain as a challenge for the application of free enzymes in biotransformations and chemical processes, are eased by the use of immobilized enzymes. During immobilization, the enzymes are anchored in a solid matrix so that the enzymes can be reused and will not be subjected to denaturation. This feature offers a wider and more economical scope for exploitation of this biocatalyst in industrial processes, waste treatment (Wada et al., 1993; Burton et al., 1998), medical science, biotechnological applications, biological fuel cells and in the development of bioprocess monitoring devices like biosensors (Ghindilis et al., 1997; Forzani and Solis, 2000). The production cost of immobilized enzymes is much lower than that of free enzymes as these can be readily separated from the reaction mixtures and hence can be used repeatedly and continuously.

Several techniques, mainly based on physical and chemical mechanisms, are applied to immobilize enzymes on solid supports. Physical methods involve the entrapment of enzyme molecules within a porous matrix (Duran and Esposito, 2000; Hussain and Jan, 2000), while chemical immobilization methods include: (i) enzyme attachment to the matrix by covalent bonds, (ii) cross-linking between enzyme and matrix, and (iii) enzyme cross-linking by multifunctional reagents. Selection of an immobilization strategy greatly influences the properties of the resulting biocatalyst. They include several parameters such as overall catalytic

* Corresponding author. Tel./fax: +91 44 24410232.
E-mail addresses: jklsac14@yahoo.co.in (L.J. Kennedy), ganesansekaran@hotmail.com (G. Sekaran).

0045-6535/$ - see front matter © 2007 Elsevier Ltd. All rights reserved.
doi:10.1016/j.chemosphere.2007.04.001

activity, effectiveness of catalyst utilization, deactivation and regeneration kinetics and the cost involved. Among the immobilization procedures, entrapment is the most suitable process for ensuring high activity of immobilized enzymes but sometimes it suffers with the leaching of enzymes from the matrix (Amsden and Turner, 1999), owing to the development of weak bonding. The stability of the immobilized enzymes depends on the strength of the electrostatic or hydrogen bonds formed between the support matrix and enzymes. Physical processes are simple and economically viable.

Among the available enzymes, polyphenol oxidase (PPO) finds extensive application in the field of biosensors (Forzani and Solis, 2000), waste water treatment, removal of toxic compounds (Wada et al., 1993; Burton et al., 1998), production of biologically active catecholamines, control of rancidification process in olive oil (Campenalla et al., 1999) and production of L-DOPA (Gayatri et al., 2002).

Various solid matrices such as cellulose, collagen membranes, polyacrylamide gel, Enzacryl AA, nylon tubing (Pialis et al., 1996), glass beads (Estrada et al., 1993), graphite electrode (Yaropolov et al., 1995), magnetite (Wada et al., 1992), gelatin gels (Wada et al., 1995), zeolite (Gayatri et al., 2002), sepiolite (Estrada et al., 1991), bentonite, chitin, chitosan and teflon membrane (Jie et al., 2004) have been considered for immobilization of PPO. Most of the studies have concluded that enzymes in inorganic carriers are more stable than those attached with organic polymers. Previous researchers proved that porous materials have favoring features for immobilizing PPO compared to non porous materials owing to their uniform and adjustable pore size, large surface area, pore volume and opened structures (Vieira and Fatibello-Filho, 1997). Therefore, in the present investigation, the feasibility for immobilization of PPO onto two inorganic mesoporous carbon matrices, one with high surface area MAC400 and the other with low surface area MAC200, has been explored. The experimental data were fitted to the non-linear form of pseudo first order, pseudo second order, and intraparticle diffusion kinetic models and also to the non-linear forms of Langmuir, Freundlich and Redlich–Peterson isotherm models.

2. Materials and methods

2.1. Adsorbents

Two mesoporous activated carbons, MAC400 and MAC200, having different physio-chemical properties as shown in the Table 1 were selected for immobilization of PPO. MAC400 and MAC200 were derived from rice husk using phosphoric acid activation at 800 °C after carbonization at 400 °C. The preparation of the carbon matrices was reported by the authors elsewhere (Kennedy et al., 2004). The mesoporous activated carbon (MAC) of size 600 μm was washed well with deionised water several times to remove soluble inorganic compounds. The washed MACs were oven dried at 120 °C for 10 h to drive off the moisture and stored in glass bottles for further use.

Table 1
Characteristics of MACs used for immobilization of PPO

S. No.	Parameter	Values	
		MAC400	MAC200
1	BET surface area ($m^2\ g^{-1}$)	439	218
2	Average pore diameter (Å)	35.3	21.4
3	Carbon (%)	38	48.4
4	Hydrogen (%)	2.4	0.70
5	Nitrogen (%)	0.50	0.10
6	Ash content (%)	59.1	50.8
7	Bulk density ($g\ cm^{-3}$)	0.56	0.69
8	Point of zero charge (PZC)	6.6	5.2
9	Moisture content (%)	14.3	8.3

2.2. Reagents

Ammonium sulphate, sodium fluoride, L-Dopa, citric acid, tri-sodium citrate-2 hydrate and all other chemicals/reagents were of analytical grade, obtained from E-Merck, Bombay, India. Commercial grade potato obtained from the local vegetable market was used as the source for enzyme extraction.

2.3. Extraction of polyphenol oxidase from potato

The polyphenol oxidase enzyme extract was prepared as per the procedure reported by Dean (1999) from *Solanum tuberosum* (potato). Five hundred grams of washed, peeled and chopped potatoes was suspended in 500 ml of cold 0.1 M sodium fluoride solution. They were homogenized using a blender, followed by filtering through a cheese filter. An equal volume of 50% saturated ammonium sulphate was added to this filtrate to precipitate PPO. It was allowed to settle for 2 h and the clear supernatant was siphoned off. The settled PPO precipitate was centrifuged at 8000 rpm for 10 min at 4 °C using a Himac C12 22G high-speed refrigerated centrifuge. The settled solid product was dissolved in 0.1 M citrate buffer (pH 4.8) and recentrifuged at 8000 rpm for 5 min at 4 °C. The supernatant containing the PPO enzyme was used for further studies.

2.4. Assay of PPO activity

PPO activity was determined by measuring the initial rate of dopachrome formation from the substrate L-Dopa, as indicated by an increase in absorbance at 475 nm (Duckworth and Coleman, 1970) using a Schimadzu UV–Visible spectrophotometer. One unit of PPO activity was defined as the amount of enzyme that caused a change in absorbance of 0.001 per minute at 25 °C for the sample containing 2.5 ml of 8 mM L-Dopa solution in 0.1 M citrate buffer along with 0.5 ml of the enzyme solution. A sample containing 2.5 ml of citrate buffer with 0.5 ml of enzyme extract was treated as the blank.

2.5. Optimization of working parameters

The stable pH range of free enzyme was determined by evaluating the enzyme activity at different pH values varying from 3 to 10. The pH of the free enzyme obtained from single batch extraction was adjusted using HCl/NaOH solution and the activity was determined at its corresponding pH. The temperature for immobilization was chosen to be 10, 20, 30, 40 °C and the enzyme activity at which maximum immobilization capacity attained was determined using enzyme activities of 5×10^4, 10×10^4, 20×10^4 and 30×10^4 U l^{-1}.

2.6. Adsorption isotherms

Langmuir, Freundlich and Redlich–Peterson (R–P) adsorption isotherms were used to determine the immobilization constants. The immobilization isotherms of PPO onto MAC400 and MAC200 were fitted at four different pH 5, 6, 7, 8, and at four different temperatures 10, 20, 30, 40 °C. The initial activities of PPO selected were 5×10^4, 10×10^4, 20×10^4 and 30×10^4 U l^{-1}. The immobilization experiment was performed in 100 ml conical flasks and the contents were agitated at 100 rpm at preset temperature for 90 min in order to attain equilibrium. The mass of MAC to volume of PPO used was 0.15 g per 10 ml for both MAC400 and MAC200. The aqueous samples were withdrawn at preset time intervals and centrifuged, followed by measuring the PPO activity using a spectrophotometer at wavelength (λ_{max}) 474, 477, 476 and 476 nm corresponding to pH 5, 6, 7 and 8, respectively.

2.7. Determination of kinetic parameters of immobilized PPO in MAC400 and MAC200

PPO activity measurement was made for different substrate concentrations at constant temperature and pH to determine kinetic parameters, maximum reaction rate (V_{max}) and Michaelis–Menten constant (K_m) for free and immobilized PPO in MAC400 and MAC200. L-tyrosine was used as the substrate and the resulting product (L-DOPA) concentration was determined by the Arnow standard method (Arnow, 1937). The kinetic parameters were estimated from the Michaelis–Menten equation,

$$V = \frac{[S]V_{max}}{[S] + K_m} \quad (1)$$

where $[S]$ is the substrate concentration (mM) and V is the initial reaction rate of the enzyme (mM min^{-1}).

2.8. FT-IR spectroscopy and scanning electron microscopy (SEM)

The surface functional groups of MAC400 and MAC200 samples were scanned using a Perkin–Elmer FT-IR spectrophotometer in the spectral range 4000–400 cm^{-1}. The surface morphology of MAC and PPO immobilized MAC samples were determined using a Leo–Jeol scanning electron microscope at the desired magnification.

3. Results and discussion

3.1. Effect of time

The effect of time for immobilization of PPO was carried out in order to determine the equilibrium points. It was found that for all experiments, the immobilization was rapid up to 20 min and then followed an asymptotic approach to equilibrium around 90 min, as shown in Fig. 1. Initially the number of adsorption sites available is higher and the driving force for the mass transfer is greater. As the immobilization time was increased the number of bare active sites became less and the PPO molecules may become clustered inside the carbon particles, thus impairing the diffusion of PPO. This may be a plausible explanation for the observed decrease in the immobilization capacity after 20 min for both MAC400 and MAC200.

3.2. Effect of pH

The stable pH for free PPO was screened by determining its activity in the pH range 3–10. A bell shaped curve was obtained, showing the PPO activity nearly constant in the pH range 6–8. The activity of the enzyme was low below

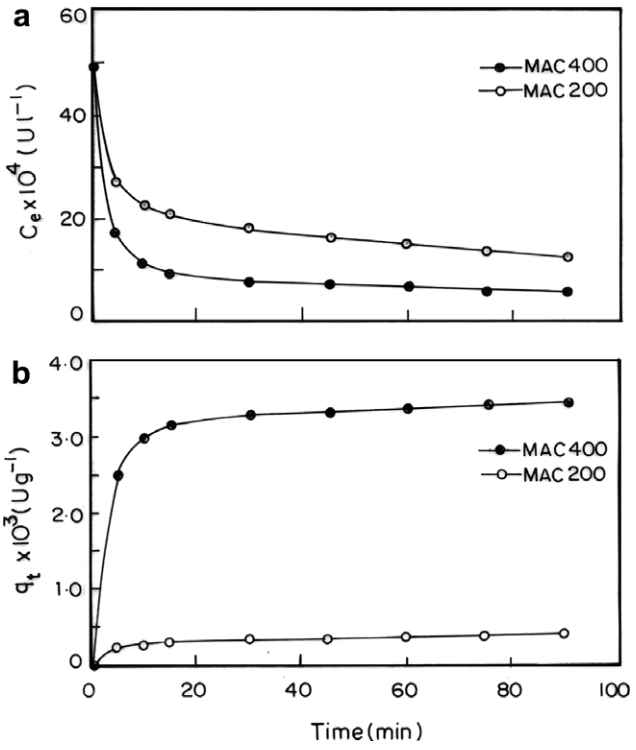

Fig. 1. (a) Activity decay curve for PPO immobilization and (b) PPO immobilization intensity with respect to time for MAC400 and MAC200 samples. (Conditions: pH 5, temperature 40 °C, activity 5×10^4 U l^{-1}.)

pH 5 and above pH 8. Hence, the effect of pH on immobilization of PPO in MAC400 and MAC200 was studied in the pH range between 5 and 8. The immobilization efficiency of PPO onto MAC400 and MAC200 with respect to pH was in the order of $5 > 6 > 7 > 8$. The decrease in immobilization capacity with increase in pH is found to be influenced by the surface charge on the adsorbent. The point of zero charge (PZC) value of MAC400 and MAC200 is 6.6 and 5.2, respectively. At a pH value below PZC, the carbon adsorbent has a net positive charge and at pH value above PZC the carbon has a net negative charge. Therefore, at $pH > pH_{PZC}$ the decrease in adsorption is observed due to electrostatic repulsion between the negatively charged adsorbent surface and the PPO species. The immobilization capacity of PPO in MAC400 and MAC200 at various pH values is shown in Fig. 2.

3.3. Effect of temperature

The immobilization capacity of PPO onto MAC400 and MAC200 increased with increase in temperature from 10 to 40 °C as shown in Fig. 3. The increase in immobilization capacity with temperature is an indication of an endothermic process involved in immobilization of PPO onto MAC. The increase in temperature may also favor the altered conformation of already adsorbed PPO on the active sites of MAC due to the acquired vibrational energy, making room for further immobilization of new PPO molecules.

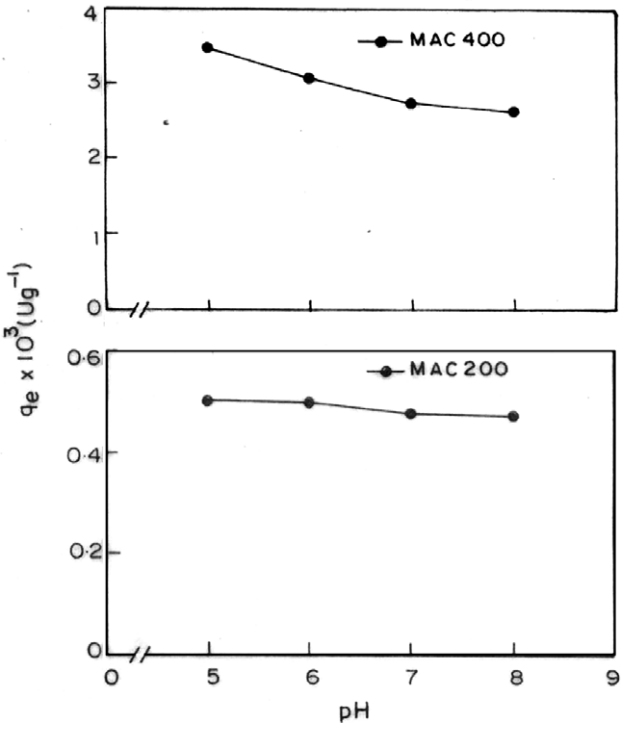

Fig. 2. Amount of PPO immobilized with respect to pH for MAC400 and MAC200 samples. (Conditions: temperature 40 °C, activity 5×10^4 U l^{-1}.)

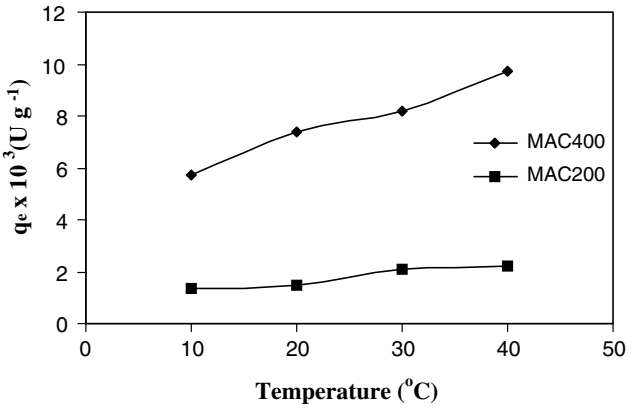

Fig. 3. Effect of temperature on the PPO immobilization on MAC400 and MAC200 samples. (Conditions: pH 5, activity 30×10^4 U l^{-1}.)

3.4. Effect of initial enzyme activity

The immobilization capacity of MAC400 and MAC200 increased with increasing PPO activity. At 40 °C, as the initial PPO activity was increased from 5×10^4 U l^{-1} to 30×10^4 U l^{-1}, the immobilization capacity increased from 3.48×10^3 to 9.71×10^3 U g^{-1} for MAC400 and from 0.50×10^3 to 2.23×10^3 U g^{-1} for MAC200. Although the immobilization capacity increased with increase in PPO activity, the percentage of immobilization decreased with increase in PPO activity. It is observed that at all concentrations studied, the immobilization capacity of MAC400 was higher than that of MAC200. This can be attributed to the difference in pore size and its distribution and the surface area.

3.5. Equilibrium isotherms

In the present study the experimental data of PPO equilibrium isotherms were studied at different pH, different concentration and different temperature, using Langmuir, Freundlich and Redlich–Peterson models because each proposed mathematical model assumes a set of hypothesis to predict the immobilization process.

$$q_e = \frac{K_L C_e}{1 + bC_e} \tag{2}$$

$$q_e = K_F C_e^{1/n} \tag{3}$$

$$q_e = \frac{K_{RP} C_e}{1 + bC_e^{\beta}} \tag{4}$$

where q_e is the solid phase sorbate concentration at equilibrium (U g^{-1}), C_e is the liquid phase sorbent concentration at equilibrium (U l^{-1}), K_L is the Langmuir isotherm constant (l g^{-1}), b is the Langmuir isotherm constant (l U^{-1}), K_F is the Freundlich constant (U g^{-1}) (l U^{-1})$^{1/n}$ and $1/n$ is the heterogeneity factor, K_{RP} is isotherm constant (l g^{-1}), b is the R–P isotherm constant (l U^{-1})$^{\beta}$ and β is the exponent that lies between 0 and 1.

Table 2
Langmuir, Freundlich and Redlich–Peterson isotherm constants for the adsorption of PPO on to MAC200 and MAC400 samples at pH 5

Sample	Temp (°C)	Langmuir model					Freundlich model				Redlich–Peterson model				
		$Q_0 \times 10^2$ (U g^{-1})	$b \times 10^{-5}$ (l U^{-1})	K_L (l g^{-1})	χ^2	R^2	K_F ((U g^{-1}) (l U^{-1})$^{1/n}$)	$1/n$	χ^2	R^2	K_{RP} (l g^{-1})	$b \times 10^{-5}$ (l U^{-1})$^{\beta}$	β	χ^2	R^2
MAC200	10	18.8	1.44	0.03	0.43	0.998	1.76	0.56	0.50	0.995	0.04	8.69	0.67	0.32	0.998
	20	20.3	1.52	0.03	0.77	0.994	2.01	0.52	0.63	0.993	0.06	32.12	0.75	0.36	0.997
	30	24.1	2.16	0.05	0.56	0.991	4.12	0.50	0.52	0.996	0.09	96.19	0.72	0.38	0.996
	40	27.1	3.33	0.09	0.83	0.994	8.90	0.48	0.72	0.994	0.18	260	0.68	0.22	0.992
MAC400	10	63.2	7.66	0.48	0.16	0.992	516	0.20	3.61	0.964	0.49	7.78	0.99	0.16	0.992
	20	78.4	9.92	0.78	0.09	0.998	396	0.11	4.52	0.838	0.77	9.96	0.99	0.09	0.998
	30	89.9	11.0	0.99	0.07	0.997	417	0.22	6.29	0.812	1.01	11.1	0.99	0.06	0.997
	40	106	21.3	2.25	0.13	0.994	573	0.36	7.45	0.802	2.25	21.3	0.99	0.13	0.994

For all the isotherms studied, the best-fit equilibrium model was determined based on chi-square, χ^2 and the correlation coefficient, R^2 using non-linear regression methods. It is observed from Table 2 that the immobilization data for MAC400 fits the Langmuir model with an average higher correlation coefficient greater than 0.99, compared to Freundlich model which has R^2 values ranging from 0.80 to 0.96. Also the values of χ^2 were low compared to that of the Freundlich model. This suggests that the immobilization of PPO onto MAC400 occurs in a monolayer form and rules out the possibility of multilayer adsorption. This is also confirmed by the three-parameter model (R–P) with regression coefficients above 0.99 and β values equal to 0.99. Thus, the higher value of β approaching 1 suggests the Langmuir model of adsorption. The adsorption isotherms are shown in Fig. 4. For MAC400 it is observed that the best fitting models of the experiments are the Langmuir and Redlich–Peterson isotherms which overlap each other. The immobilization capacity of MAC400, was observed to be higher than that of MAC200. The pore size of the MAC400 having an average pore diameter 35.3 Å, enabled the enzyme molecules easy access to the pores leading to an increased immobilization capacity. The immobilization of the enzyme molecules onto MAC400 may involve a series of steps. First, the enzyme molecules migrate from the bulk phase to the carbon matrix by diffusion. Second, the enzyme molecule is linked with unsaturated bonded sites of the mesopore through electrostatic interaction. The immobilized molecules undergo compression and refolding so as to accommodate fresh entries. Finally the enzymes enter the inner sites of mesopores and get entrapped by establishing bond with the walls of the pores.

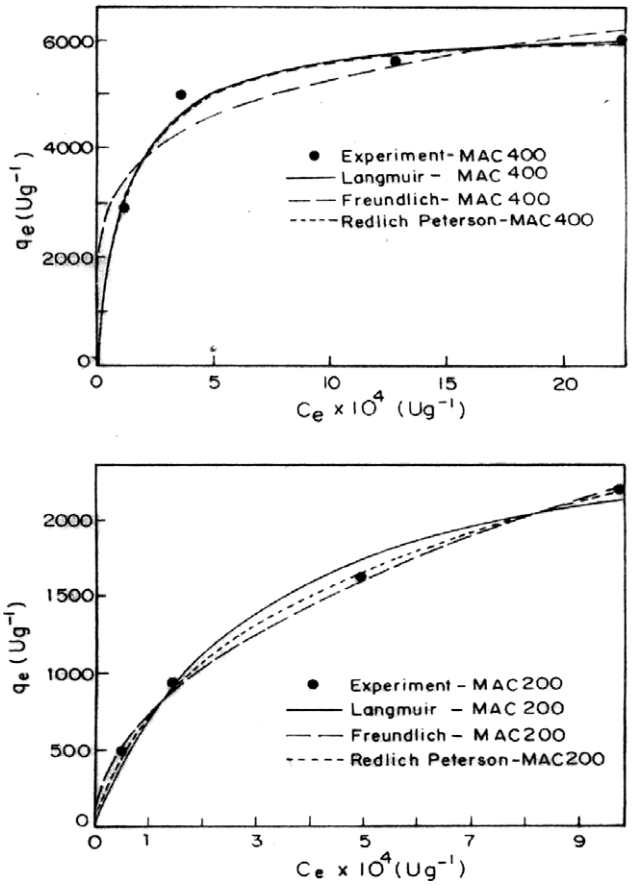

Fig. 4. Langmuir, Freundlich and Redlich Peterson isotherm plots for the immobilization of PPO on to MAC400 and MAC200 carbon samples. (Conditions: pH 5, temperature 20 and 40 °C, respectively.)

For MAC200, it is observed that the correlation coefficient R^2 was greater than 0.99 with low chi-square (χ^2) for both Langmuir and Freundlich isotherm models. This suggests the occurrence of both monolayer and multilayer adsorption of PPO onto MAC. The mixed response for monolayer and multilayer adsorption is evident from β values obtained in the range of 0.67–0.75 with regression coefficients above 0.99. The MAC200 has lower adsorption capacity due to the average pore diameter of 21.4 Å. This pore dimension is inadequate for the PPO enzyme molecule to diffuse into the pores freely. Under circumstances where the molecular size of enzyme is large enough to enter into the pores, multilayer adsorption onto outer pore surface area takes place (Goradia et al., 2005). Multilayer adsorption is largely confined to the external pore surface area of the activated carbon and is evident from the SEM photograph of MAC200 and MAC400 immobilized with PPO. Clustering of the enzyme molecules at the pore entrance

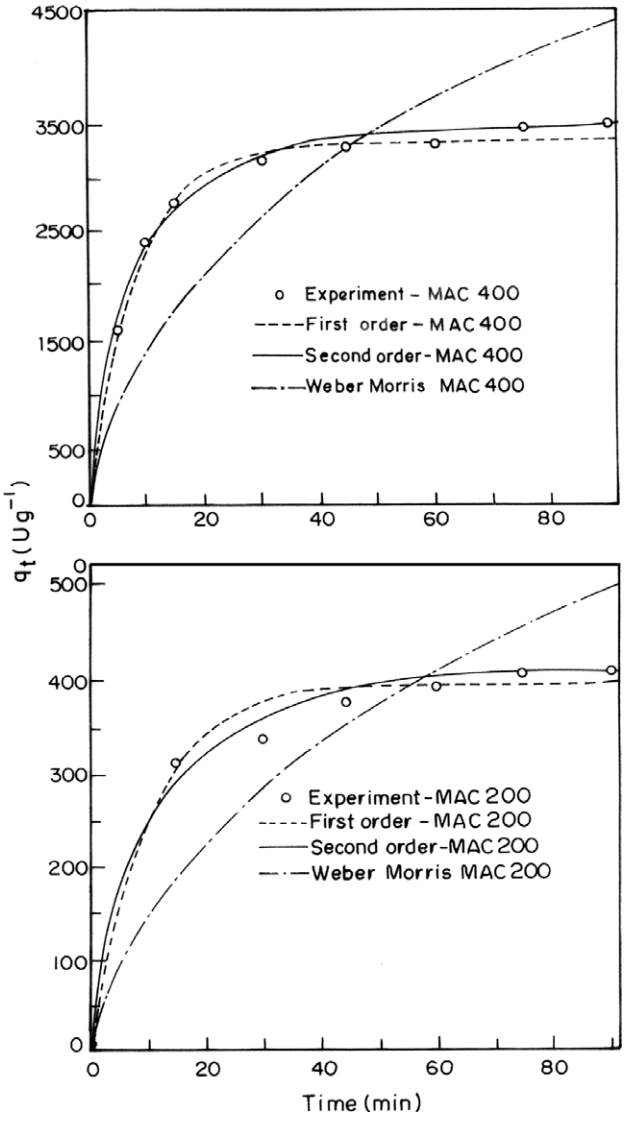

Fig. 5. Pseudo first order, pseudo second order and Weber–Morris plots for PPO immobilization on to MAC400 and MAC200 carbon samples. (Conditions: pH 5, temperature 40 °C, activity 5×10^4 U l^{-1}.)

is a plausible explanation for the reduced amount of immobilization onto MAC200 at higher PPO loading, which could clog the channels so that PPO enzyme is unable to get into the pores. Thus, it may be concluded that multilayer adsorption occurs at high concentration and monolayer adsorption occurs at very low concentration of PPO.

3.6. Adsorption kinetic modeling

The non-linear forms of the pseudo first order model (Eq. (5)) (Lagergren and Svenska, 1898), pseudo second order kinetic model (Eq. (6)) (Ho and McKay, 1998) and intraparticle diffusion model (Eq. (7)) (Weber and Morris, 1963) were applied to the experimental data at different temperatures, concentrations and pH.

$$q_t = q_e(1 - \exp^{-k_1 t}) \tag{5}$$

$$q_t = \frac{k_2 q_e^2 t}{1 + k_2 q_e t} \tag{6}$$

$$q_t = k_p t^{1/2}, \tag{7}$$

where q_e and q_t are the amount of PPO immobilized onto MAC at equilibrium and at time t, (U g^{-1}), k_1, k_2 and k_p are the pseudo first, second order and pore diffusion rate constants.

The validity of the order of adsorption processes is based on two criteria, the first based on the regression coefficients and the second based on predicted q_e values. The first order rate constant k_1, the second order rate constant k_2 and pore diffusion constant k_p were evaluated with data fits shown in Fig. 5. The correlation coefficients for the first order kinetic model for MAC400 and MAC200 were in the range 0.63–0.96 and 0.80–0.97, respectively. Also the predicted q_e values for both the MAC400 and MAC200 obtained from the first order kinetic model were not very close to the experimental values as shown in the Table 3. This indicates that the immobilization of PPO onto MAC200 and MAC400 does not follow the first order kinetic model. But for the case of the pseudo second order kinetic model, it was observed that the correlation coefficients were greater than 0.99 with the predicted q_e values in good agreement with the experimental q_e values, as seen in Table 3. Thus, it is inferred that the immobilization of

Table 3
Comparison of the first and second order rate constants with experimental and predicted q_e values for PPO adsorption on to samples (MAC400 and MAC200) at different pH (conditions: activity: 20×10^4 U l^{-1}, temperature 40 °C)

Parameter		First order kinetic model				Second order kinetic model		
Sample	pH	$q_e \times 10^2$ (U g^{-1}) (experimental)	$q_e \times 10^2$ (U g^{-1}) (predicted)	k_1 (min^{-1})	R^2	$q_e \times 10^2$ (U g^{-1}) (predicted)	$k_2 \times 10^{-5}$ (g U^{-1} g^{-1} min^{-1})	R^2
MAC400	5	130	110	0.06	0.934	129	4.21	0.999
	6	82.0	71.3	0.06	0.738	81.1	3.43	0.998
	7	73.2	64.3	0.06	0.632	70.2	2.72	0.993
	8	61.0	58.2	0.05	0.96	60.9	1.90	0.997
MAC200	5	12.8	11.0	0.05	0.918	12.5	12.1	0.998
	6	11.3	10.1	0.08	0.973	11.0	10.4	0.999
	7	11.0	9.86	0.06	0.967	10.0	9.31	0.997
	8	10.2	7.26	0.05	0.804	9.96	8.49	0.996

PPO onto MAC system belongs to second order kinetic model.

The intraparticle diffusion model proposed by Weber and Morris (Weber and Morris, 1963) also did not fully fit the adsorption data of PPO in both the MACs as it possessed very low regression coefficients, less than 0.49.

3.7. Enzyme kinetic parameters

Kinetic parameters, K_m and V_{max} for free and immobilized enzymes were calculated from the Michaelis–Menten plot (Fig. 6). The K_m values signify the extent to which the enzymes have access to the substrates (Shuler and Kargi, 2005). The lower value of K_m represents higher affinity between enzymes and substrates. It is observed that PPO immobilized in MAC400 (PPO–MAC400) has slightly lower K_m (0.41 mM) value than the free enzyme (0.49 mM) indicating higher affinity of the PPO–MAC400 towards substrate tyrosine (enzyme–substrate complex formation) compared to that of PPO–MAC200, which has K_m value (0.65 mM) higher than others. The higher value of PPO–MAC200 indicates that enzyme and substrate do not prefer to come together for a long time. The V_{max} values of PPO–MAC400 and PPO–MAC200 are 0.01 and 0.04 mM min^{-1}, respectively while for the free enzyme it is 0.05 mM min^{-1}. The low value of V_{max} for both the immobilized matrices indicates the difficulty of enzyme substrate interaction. The V_{max} values are in the order of PPO > PPO–MAC200 > PPO–MAC400. This suggests that the immobilized PPO in MAC400 has more affinity towards the substrate and the enzyme is less active in catalyzing the diphenol formation. This is evident from the ratio of V_{max}/K_m values for free enzyme, PPO–MAC200 and PPO–MAC400, with values of 0.11, 0.06 and 0.02 min^{-1}, respectively. The greater the V_{max}/K_m value, the higher the catalytic efficiency of the enzyme for the substrate. The kinetic parameters determined suggest that the catalytic efficiency is in the order of PPO–MAC < PPO while the substrate interaction efficiency of PPO–MAC200 is greater than that of PPO. The efficiencies of PPO–MAC400 and PPO–MAC200 illustrate that the enzyme molecule in MAC200 is less strongly held without affecting the conformation of PPO, while in MAC400 the enzymes are loaded with altered conformation (strained condition) leading to retardation of catalytic efficiency. The catalytic efficiency of the enzyme depends on the rate at which the active oxy form of PPO is formed from the meta form. The transformation of the meta to the oxy through the deoxy form is favored under limited oxygen supply. This condition is more facilitated in MAC200 as it is evidenced through the formation of oxy functionalized groups in MAC200.

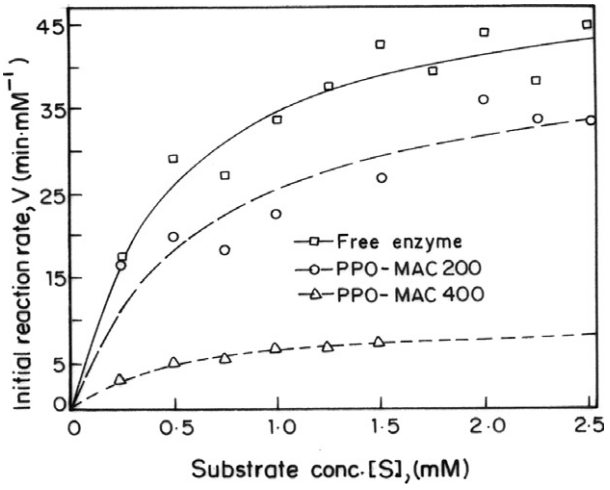

Fig. 6. Michaelis–Menten plots of free and immobilized PPO enzyme on MAC400 and MAC200 samples.

3.8. Shelf-life of enzyme/carbon matrix

To determine the shelf-life of the enzyme/carbon matrix, the activity of the PPO–MAC400 was checked at an interval of 2 days and continued for 40 days. For PPO immobilized carbons, the enzyme activity remained constant with small fluctuations, perhaps due to change in conformation of enzyme (Ahu et al., 2005).

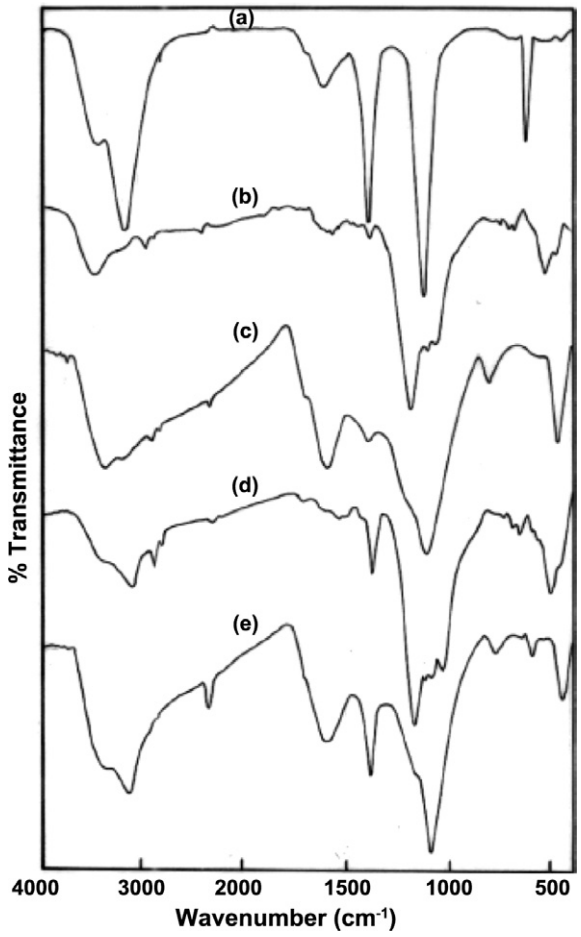

Fig. 7. FT-IR spectrum of (a) PPO, (b) MAC400, (c) MAC200, (d) PPO–MAC400 and (e) PPO–MAC200 samples.

3.9. Fourier transform infrared spectra (FT-IR)

The infrared spectra for PPO, MAC400, MAC200, PPO–MAC400 and PPO–MAC200 are shown in Fig. 7. MAC400 and MAC200 have a wide band at about 3400–3425 cm^{-1} due to O–H stretching mode of hexagonal groups and adsorbed water. The position and symmetry of this band at lower wave numbers indicate the presence of strong hydrogen bonds. For MAC400 and MAC200, an absorption band is observed at 2920 cm^{-1} due to aliphatic C–H stretching. The broad peak shouldered at about 1180 cm^{-1} indicates the presence of phosphorous content of MAC400. The broad peak shouldered at about 1100 cm^{-1} and peaks near 800 and 475 cm^{-1} indicate the presence of silica for both MAC400 and MAC200 samples.

The FT-IR spectrum of powdered PPO contains two broad bands near 3200–3400 cm^{-1} and is due to N–H stretching frequencies. This can be assigned to primary amines, as there are two bands owing to N–H asymmetric and N–H symmetric stretching. A band near 1631 cm^{-1} corresponds to N–H inplane bending while two sharp bands at 1400 and 1121 cm^{-1} correspond to C–N stretching frequencies. A sharp band at 619 cm^{-1} corresponds to the C–H out of plane bending.

The band near 3135 cm^{-1} in PPO has been shifted to 3143 cm^{-1} in PPO–MAC400 and to 3155 cm^{-1} in PPO–MAC200, indicating stronger bonding of PPO with the functional groups of MAC. The N–H stretching frequency in the region 3200–3500 cm^{-1} is observed by the appearance of two bands for PPO–MAC400 and PPO–MAC200 compared to only one band for MAC200 and MAC400. The appearance of these bands is due to the molecular interaction of PPO with activated carbon matrices. The decrease in the broadness of the peak is well observed in PPO–MAC400 rather than PPO–MAC200 and indicates that PPO is strongly immobilized in MAC400 as opposed to MAC200. The band corresponding to 1400 cm^{-1} due to C–N stretching vibrations, observed in both the PPO immobilized carbons, confirms the presence of PPO immobilized in the matrices. These bands were absent in MAC400 and MAC200 matrices.

3.10. Scanning electron microscopy (SEM)

The surface morphology of MAC400, MAC200, PPO–MAC400 and PPO–MAC200 matrices are shown in Fig. 8a–d. The micrographs reveal that MAC400 and MAC200 are highly porous in nature with differences in pore size. It is observed that in PPO–MAC200, the PPO immobilization was minor while in PPO–MAC400, PPO is well immobilized inside the pores of the carbon matrix. The enzyme is also located at the outer pore surface area of activated carbon. This sort of pore penetration of PPO in MAC400 is not observed in MAC200. This can be attributed to the decreased average pore size (21.4 Å) of MAC200.

The immobilization of PPO in MAC400 is evident from Fig. 8c. It is seen in the photo that the enzymes are stuck or

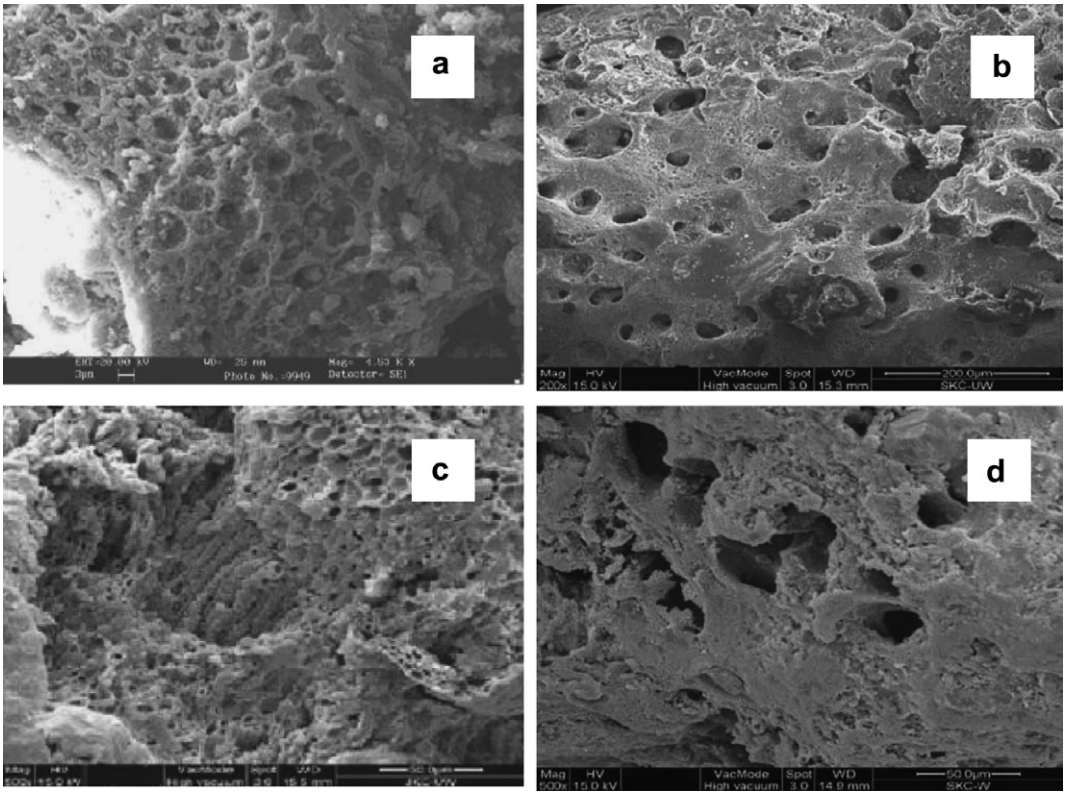

Fig. 8. Micrograph showing (a) surface morphology of highly porous MAC400, (b) MAC200, (c) PPO–MAC400, (d) PPO–MAC200 samples.

bound to the inner wall of the pores in the carbon matrix. Due to this, the pore wall surfaces are fully modified. The enzymes enter into the deep pores of the carbon matrix and after filling the pores the enzyme resides at the entrance of the mouth of the pores in the carbon matrix. Certain pores are completely vacant in PPO–MAC and the unoccupied pores are clearly exhibited in the background of the immobilized carbon samples.

4. Conclusions

Detailed studies performed with two different carbon matrices suggested that MAC400 is an ideal matrix for immobilization of PPO as compared to MAC200. The optimum conditions for immobilization of PPO onto MAC400 and MAC200 are temperature 40 °C, pH 5 and at PPO activity equal to 30×10^4 U l^{-1}. MAC400 followed the Langmuir mode of adsorption while MAC200 followed both the Langmuir and Freundlich models, suggesting the occurrence of both monolayer and multilayer adsorption. The second order rate equation was followed for the immobilization process. Kinetic parameters for free and immobilized enzymes, determined according to the Michaelis–Menten equation, showed a lower K_m value for PPO–MAC400 than the free enzyme, indicating higher affinity towards substrate, while PPO–MAC200 exhibited a higher K_m value. FT-IR spectra provide evidence of the PPO enzyme immobilized onto the carbon matrices. The PPO immobilized/carbon morphology was observed in the SEM photographs.

Acknowledgement

The first and the other co-authors highly thank the corresponding author Dr. G. Sekaran, Deputy Director and Head, Dept. of Env. Tech, C.L.R.I, for providing financial assistance and support to carry out the work.

References

Ahu, A., Senem, K., Levent, T., Yusuf, Y., 2005. Immobilization of tyrosinase in polysiloxane/polypyrrole copolymer matrices. Int. J. Biol. Macromol. 35, 163–167.

Amsden, B., Turner, N., 1999. Diffusion characteristics of calcium alginate gels. Biotechnol. Bioeng. 65, 605–610.

Arnow, L.E., 1937. Colorimetric determination of the components of 3,4 dihydroxy phenylalanine–tyrosine mixture. J. Biol. Chem. 118, 531–537.

Burton, S.G., Boshoff, A., Edwards, W., Rose, P.D., 1998. Biotransformation of phenols using immobilized polyphenoloxidase. J. Mol. Catal. B: Enzym. 5, 411–416.

Campenalla, L., Favero, G., Pastorino, M., Tomasetti, M., 1999. Monitoring the rancidification process in olive oils using a biosensor operating in organic solvents. Biosens. Bioelectron. 14, 179–186.

Dean, R.L., 1999. A commentary on experiments with tyrosinase. Am. Biol. Teach. 61 (7), 523–527.

Duckworth, H.W., Coleman, J.E., 1970. Physiochemical and kinetic properties of mushroom tyrosinase. J. Biol. Chem. 245, 1613–1625.

Duran, N., Esposito, E., 2000. Potential applications of oxidative enzymes and phenol oxidase-like compounds in wastewater and soil treatment: a review. Appl. Catal. B: Environ. 28, 83–99.

Estrada, P., Sanchez-Muniz, R., Acebal, C., Arche, R., Castillon, M.P., 1991. Characterization and optimization of immobilized polyphenoloxidase in low-water organic solvents. Biotechnol. Appl. Biochem. 14, 12–20.

Estrada, P., Baroto, W., Castillon, M.P., Acebal, C., Arche, R., 1993. Temperature effects on polyphenoloxidase activity in organic solvents with low water content. J. Chem. Technol. Biotechnol. 56, 59–65.

Forzani, E.S., Solis, V.M., 2000. Electrochemical behaviour of polyphenoloxidase immobilized in self-assembled structures layer by layer with cationic polyallylamine. Anal. Chem. 72, 5300–5307.

Gayatri, S., Bradley, A.S., 2002. L-Dopa production from tyrosinase immobilized on zeolite. Enzyme Microb. Technol. 31, 747–753.

Ghindilis, A.L., Atanosov, P., Wilkins, F., 1997. Enzyme catalysed electron transfer: fundamentals and analytical applications. Electroanalysis 9, 661–673.

Goradia, D., Cooney, J., Hodnett, B.K., Magner, E., 2005. The adsorption characteristics, activity and stability of trypsin onto mesoporous silicates. J. Mol. Catal. B: Enzym. 32, 231–239.

Ho, Y.S., McKay, G., 1998. Sorption of dye from aqueous solution by peat. Chem. Eng. J. 70, 115–124.

Hussain, Q., Jan, U., 2000. Detoxification of phenols and aromatic amines from polluted wastewater by using polyphenol oxidases. J. Sci. Ind. Res. 59, 286–293.

Jie, L., Jei, F., Chengzhong, Y., Luyan, Z., Shiyi, J., Bo, T., Dongyuan, Z., 2004. Immobilization of enzymes in mesoporous materials: controlling the entrance to nanospace. Micropor. Mesopor. Mater. 73, 121–128.

Kennedy, L.J., Judith, V.J., Sekaran, G., 2004. Effect of two stage process on the preparation and characterization of porous carbon composite from rice husk by phosphoric acid activation. Ind. Eng. Chem. Res. 43, 1832–1838.

Lagergren, S., Svenska, B.K., 1898. Zur theorie der sogenannten adsorption geloester stoffe. Veternskapsakad Handlingar 24, 1–39.

Palmer, T., 1991. Understanding Enzymes. Prentice-Hall, New York.

Pialis, P., Hamann, M.C.J., Saville, B.A., 1996. L-Dopa production from tyrosinase immobilized on nylon 6,6. Biotechnol. Bioeng. 51, 141–147.

Shuler, M.L., Kargi, F., 2005. Bioprocess Engineering-Basic Concepts. Prentice-Hall, India.

Vieira, I.C., Fatibello-Filho, O., 1997. Amperometric biosensor for the determination of phenols using a crude extract of sweet potato (*Ipomea batata*). Anal. Lett. 30, 895–907.

Wada, S., Ichikawa, H., Tatsumi, K., 1992. Removal of phenols with tyrosinase immobilized on magnetite. Water Sci. Technol. 26, 2057–2059.

Wada, S., Ichikawa, H., Tatsumi, K., 1993. Removal of phenols from wastewater by soluble and immobilized tyrosinase. Biotechnol. Bioeng. 42, 854–858.

Wada, S., Ichikawa, H., Tatsumi, K., 1995. Removal of phenols and aromatic amines from wastewater by a combination treatment with tyrosinase and a coagulant. Biotechnol. Bioeng. 45, 304–309.

Weber, W.J., Morris, J.C., 1963. Kinetics of adsorption on carbon from solutions. J. Sanit. Eng. Div. ASCE 89, 31–60.

Yaropolov, A.I., Kharybin, A.N., Emneus, J., Marko-Varga, G., Gorton, L., 1995. Flow-injection analysis of phenols at a graphite electrode modified with co-immobilized laccase and tyrosinase. Anal. Chim. Acta 308, 137–144.